Microchimica Acta
https://doi.org/10.1007/s00604-017-2656-7

ORIGINAL PAPER

Lysozyme aptasensor based on a glassy carbon electrode modified with a nanocomposite consisting of multi-walled carbon nanotubes, poly(diallyl dimethyl ammonium chloride) and carbon quantum dots

Behzad Rezaei [1] · Hamid Reza Jamei [1] · Ali Asghar Ensafi [1]

Received: 30 September 2017 / Accepted: 29 December 2017

Abstract
An aptamer-based method is described for electrochemical determination of lysozyme. A glassy carbon electrode was modified with a nanocomposite composed of multi-walled carbon nanotubes, poly(diallyl dimethyl ammonium chloride), and carbon quantum dots. The composition of the nanocomposite (MWCNT/PDDA/CQD) warrants good electrical conductivity and a high surface-to-volume ratio. The lysozyme-binding aptamers were immobilized on the nanocomposite via covalent coupling between the amino groups of the aptamer and the carboxy groups of the nanocomposite. The modified electrode was characterized by electrochemical impedance spectroscopy, cyclic voltammetry and differential pulse voltammetry. The use of this nanocomposite results in a considerable enhancement of the electrochemical signal and contributes to improving sensitivity. Hexacyanoferrate was used as an electrochemical probe to study the dependence of the peak current on lysozyme concentration. In the presence of lysozyme, the interaction of lysozyme with immobilized aptamer results in a decrease of the peak current, best measured at +0.15 V vs. Ag/AgCl. A plot of peak current changes versus the logarithm of the lysozyme concentration is linear in the 50 fmol L^{-1} to 10 nmol L^{-1} concentration range, with a 12.9 fmol L^{-1} detection limit (at an S/N ratio of 3). The method is highly reproducible, specific and sensitive, and the electrode has a rapid response. It was applied to the determination of lysozyme in egg white, serum, and urine.

Keywords Biosensor · Differential pulse voltammetry · Electrochemical aptasensor · Electrochemical impedance spectroscopy · Nanocomposite

Introduction

The quantification and detection of proteins play important roles in fundamental studies conducted on food safety [1], proteomics [2], bioengineering [3], medical, and clinical applications [4]. In this regard, the aptamer-based sensor (aptasensor) is proved to be a powerful technique for the identification of proteins, kinds of bio-molecules and biochemical reactions [5].

Lysozyme is a remarkably small protein. It is a ubiquitous enzyme and plays a vital role in various organisms [6]. It is highly effective in the defense system of the human body due to its antibacterial activity [7]. Moreover, this protein is applied in medicine and clinical fields as a tumor marker (especially for myelomonocytic leukemia), model in pharmaceutical, application in antibiotics field, model in protein studies, model for enzyme catalysis, and in proteomics [8]. It is available in nature as a single polypeptide chain that includes 129 amino acid residues with a MW of 14,300 Da, and an isoelectric point of 11.0 [8]. Given the importance of the clinical detection of lysozyme, scholars have proposed several methods such as electrophoretic [9], immune-enzymatic, chromatographic [10], ELISA [11], optical, electrochemiluminescent [12], colorimetric, surface plasmon resonance [13], and electrochemical methods [14].

Electronic supplementary material The online version of this article (https://doi.org/10.1007/s00604-017-2656-7) contains supplementary material, which is available to authorized users.

✉ Behzad Rezaei
rezaei@cc.iut.ac.ir

[1] Department of Chemistry, Isfahan University of Technology, Isfahan 84156-83111 I.R., Iran

Published online: 14 February 2018

Aptamers are short single-stranded DNA/RNA molecules and functional nucleic acid receptors which bind to specific target molecules with high affinity. They are applied for clinical goals and basic research for drugs, proteins and other inorganic/organic molecules [3]. Considerable efforts have been made to develop aptasensors using various identification methods such as colorimetric [15, 16], fluorescent [17], quartz crystal microbalance [18], surface plasmon resonance [13], field effect transistors [19], optical sensor [20], electrochemiluminescence [12], magnetic sensors [21], and electrochemical methods [14, 22].

Electrochemical aptasensors have been developed by combining aptamer-based signal conversion strategies with various electrochemical techniques to identify different targets. These methods compared to other used techniques are faster in response, more robust, sensitive, stable, cost-efficient, and suitable for miniaturization [23]. These different electrochemical methods include potentiometric, amperometric, Faradaic impedance, and voltammetric techniques [5, 24].

The most important step in making electrochemical biosensors based on aptamer is the immobilization of aptamer on the transducer surface [25] because this process not only provides a functionalized sensing interface but also ascertains the selectivity, stability, and sensitivity of the electrochemical aptasensors [26]. One of the main factors in designing electrochemical aptasensors is the development of efficient aptamer immobilization methods, which tightly fixes the aptamer and makes it stable on the electrode surface [27, 28]. Various methods, including direct adsorption or π - tacking interaction, affinity binding based on biotin-avidin, covalent coupling, sol–gel entrapment, electrostatic interaction, and self-assembled monolayers (SAMs), have been put forward for the immobilization of aptamers [8].

Considerable progress made reveals that combining aptamer with nanomaterials is successful for building and developing novel electrochemical biosensing platform in protein analysis methods, biological engineering, and clinical detection. Fabrication of novel nanostructures such as carbon quantum dots (CQD), carbon nanotubes, gold nanoparticles, and nanosheets [29], having highly improved properties, is an alluring prospect of nanotechnology in the development of sensitive, stable, and cost-effective aptasensor [30]. Carbon quantum dots (CQD) are carbon nanoparticles with small sizes less than 10 nm so that the electron wave functions are limited within their volume. They have become one of the most important nanomaterials in recent scientific research [31].

CQD can be taken into account as a potential material to enhance the immobilization of biological types (aptamer chains or DNA) because of some if its noticeable characteristics, including hydrophilicity, good chemical stability, susceptibility to chemical modifications, benignity to chemical composition, biodegradability, non-toxicity, good conductivity, biocompatibility, and cost efficiency. In addition, CQDs are appropriate for chemical modification with various biological, polymeric, organic, and inorganic materials [32–34]. Multi-walled carbon nanotubes (MWCNTs), as another class of nanoparticles, are used as a modifier in the electrochemical aptasensor [22], because they have the good conductivity, specific surface areas, and high surface-to-volume ratios for better immobilization of aptamers [22].

In this study, the combination of a nanocomposite of MWCNTs, poly diallyldimethylammonium chloride (PDDA), and CQD (MWCNT/PDDA/CQD) is proposed to improve the electrochemical aptasensor for lysozyme detection. This combination is used into an electrochemical aptasensor to apply synergy contributions for better immobilization of aptamer and improvement of aptasensor characteristics. It should be noted that PDDA (as a conductive cationic polymer) is used as a dispersant of functionalized MWCNTs. In addition, PDDA causes an electrostatic assembly between positively charged PDDA/MWCNT and negatively charged synthesized CQD [28]. Compared with other electrochemical aptasensors, the novel GCE has key advantages for the immobilization of amino-linked anti-lysozyme aptamer using amine coupling method. These advantages include rich π-conjugation structure, large surface area, excellent in-plane conductivity resulting from the presence of functionalized MWCNTs as well as positively charged PDDA, many amino and carboxy functional groups on the synthetic CQD surface, and its conductivity.

Experimental

Chemical and apparatuses

The sequence of anti-lysozyme aptamer (APT) applied in this study is "5′-NH2-ATC TAC GAA TTC ATC AGG GCT AAA GAG TGC AGA GTT ACT TAG-3". The description of all reagents and chemical materials and apparatuses are presented in more detail in the “Electronic Supporting Material” file (Section S1).

Synthesis of CQD

In the first step, 1.05 g urea and 0.90 g citric acid were dissolved into 25 mL pure water. After that, the formed solution was poured into 100 mL Teflon-lined stainless autoclave. The closed autoclave was transferred into an electric oven at 180 °C for 10 h. Then, ethanol was added to the prepared solution to get the final product. The solid product was separated by centrifuging it at 3727 g for 5 min. Then, after dissolving the solid product in pure water, the solution was filtered by filter membrane (0.22 μm) to remove the possible coarse particles and dried at room temperature.

Preparation of the MWCNT/PDDA/CQD nanocomposite

In order to purify and activate the MWCNTs, they were heated at reflux in nitric acid. In this step, 0.40 g of the MWCNTs (diameter of 70–110 nm, length of 5–9 μm bundles) were sonicated with 80 mL of HNO_3 5.0 mol L^{-1} and refluxed for 15 h. The mixture of MWCNTs was diluted with water and then was filtered. The washing procedure continued until the water layer reached a neutral pH. Then, the final product of MWCNTs was dried at room temperature. This procedure produces –COOH groups on the MWCNTs structure. In this experiment, 5.0 mg of the activated MWCNTs were dispersed with 5.0 mL of the solution including 0.5 mol L^{-1} of NaCl and 0.005 g PDDA by ultrasonication of the solution for 1.5 h. Afterward, 2 mg of synthesized CQD was added to the dispersed MWCNT/PDDA solution and the resulting suspension was sonicated for 1 h. Finally, the homogenous dispersion of MWCNT/PDDA/CQD nanocomposite was prepared.

Covalent immobilization of aptamer, and lysozyme detection

In this section, glassy carbon electrodes (GCE) were first polished with 0.05 mm of alumina slurries. After that, they were ultrasonically washed in ethanol and water 50% (*V*/V) solution and in distilled water, respectively. Then, 5.0 μL of the homogenous dispersion of MWCNT/PDDA/CQD was dropped onto a GCE surface and dried at room temperature. The carboxylic groups of MWCNTs and CQD placed on the GCE surface were activated in a mixture of 100 mM EDC (1-ethyl-3-(3-dimethylaminopropyl) carbodiimide hydrochloride) and 100 mM NHS (N-hydroxysuccinimide) in 10 mM TE buffer (pH 7.4) for 2 h. Afterward, in order to immobilize the APT covalently, the GCE-MWCNT/PDDA/CQD was immersed in TE buffer solution (pH 7.4) containing 0.1 μM aptamer for 2.5 h. Then, the electrodes were washed with TE buffer for 10s to eliminate unbound aptamers from the modified GCE. 40 μL of 0.1% BSA solution was also dropped on the prepared GCE-MWCNT/PDDA/CQD/aptamers dropped for 1 h to deactivate the remaining succinimide groups and avoid nonspecific adsorption. After being washed with TE buffer, the prepared electrode was immersed in TE buffer including lysozyme with various concentrations for 1.5 h. Each of the prepared GCEs was used once for each measurement of lysozyme protein. In order to detect changes in the electrochemical properties of the modified GCE, electrochemical methods such as differential pulse voltammetry (DPV), electrochemical impedance spectroscopy (EIS), and cyclic voltammetry (CV) were applied.

Electrochemical measurements

The modified electrode performances were evaluated by EIS, DPV, and CV in a three electrode cell assembly, having 2.5 mmol L^{-1} $[Fe(CN)_6]^{3-/4-}$ (1:1) mixture as a redox probe and 0.1 mol L^{-1} KCl in TE buffer (pH 7.4). The EIS measurements were conducted in a frequency range from 5 mHz to 100 kHz with a sinusoidal signal of 10 mV and at a DC potential of +0.15 V versus Ag/AgCl (3 M KCl). CV was applied by a potential scanning between −0.2 and 0.6 V at a scan rate of 100 mV s^{-1}. DPV was also used with following parameters modulation amplitude of 50.0 mV, step potential of 8.0 mV, modulation time of 0.05 s and interval time of 0.5 s. Using Golay and Savitzky filter (level 2) of the GPES software, the raw voltammograms of DPV method were treated. The average baseline correction was defined by a 'peak width' of 0.01 V. The measurements of CV, EIS, and DPV techniques were conducted using an AUTOLAB PGSTAT 12 device at room temperature and the GPES and FRA software version 4.9.

Results and discussion

According to the description stated in the "Introduction" section, the MWCNTs was used to development of lysozyme assay because of the various characteristics, including the good conductivity, specific surface areas, and high surface-to-volume ratios for better immobilization of aptamers, high mechanical strength, cheap fairly price, and availability. Moreover, the synthesized CQDs was used to development of lysozyme assay due to good chemical stability, susceptibility to chemical modifications, benignity to chemical composition, biodegradability, non-toxicity, good conductivity, biocompatibility, and cost efficiency. Additionally, the PDDA, as a conductive cationic polymer, was used as a dispersant of functionalized MWCNTs. It also causes an electrostatic assembly between positively charged PDDA/MWCNT and negatively charged CQDs. The MWCNT/PDDA/CQD nanocomposite was applied to development of lysozyme assay due to the high electron mobility, synergistic contribution of functional components, high specific surface, high mechanical strength, low manufacturing cost, and so forth.

Characterization of CQD

The Dynamic Light Scattering (DLS), X-ray diffraction (XRD), Fourier Transform Infrared (FT-IR), UV-vis-NIR, and fluorescence spectroscopy techniques were applied to study the characteristics of CQDs synthesized from urea and citric acid. The obtained results of this section were explained in the "Electronic Supporting Material" file (Section .S21).

Surface morphology of nanocomposites on the GCE

Field emission-scanning electron microscope (FE-SEM) is a powerful technique for investigating the morphology of a surface on a nano-scale. Figure 1 shows the surface morphologies of each modified working GCE using FE-SEM. Figure 1a clearly displays the surface roughness of unmodified GCE. Figure 1b shows the electrode coverage morphology modified with CQD/PDDA. As observed in this figure, the effective surface area of the modified GCE has increased and CQDs are dispersed in the PDDA solution. This is also an evidence of the coverage of CQDs on the surface of GCE, and an increase in the current, in the presence of this modifier. The FE-SEM images of MWCNT/PDDA film show a good dispersion in Fig. 1c. As seen in this figure, the impressive surface area of the modified GCE has increased by deploying well conductive MWCNTs compared with unmodified GCE. Figure 1d shows that the modified GCE surface of MWCNT/PDDA/CQD nanocomposite is visible and CQDs appear to enhance the surface area of nanotubes. Furthermore, CQDs were detected on the sidewalls of MWCNTs, which reveals the highly conjugated CQDs-MWCNTs hetero-junctions. Figure 1e shows the immobilization of APT on the GCE surface modified with MWCNT/PDDA/CQD nanocomposite.

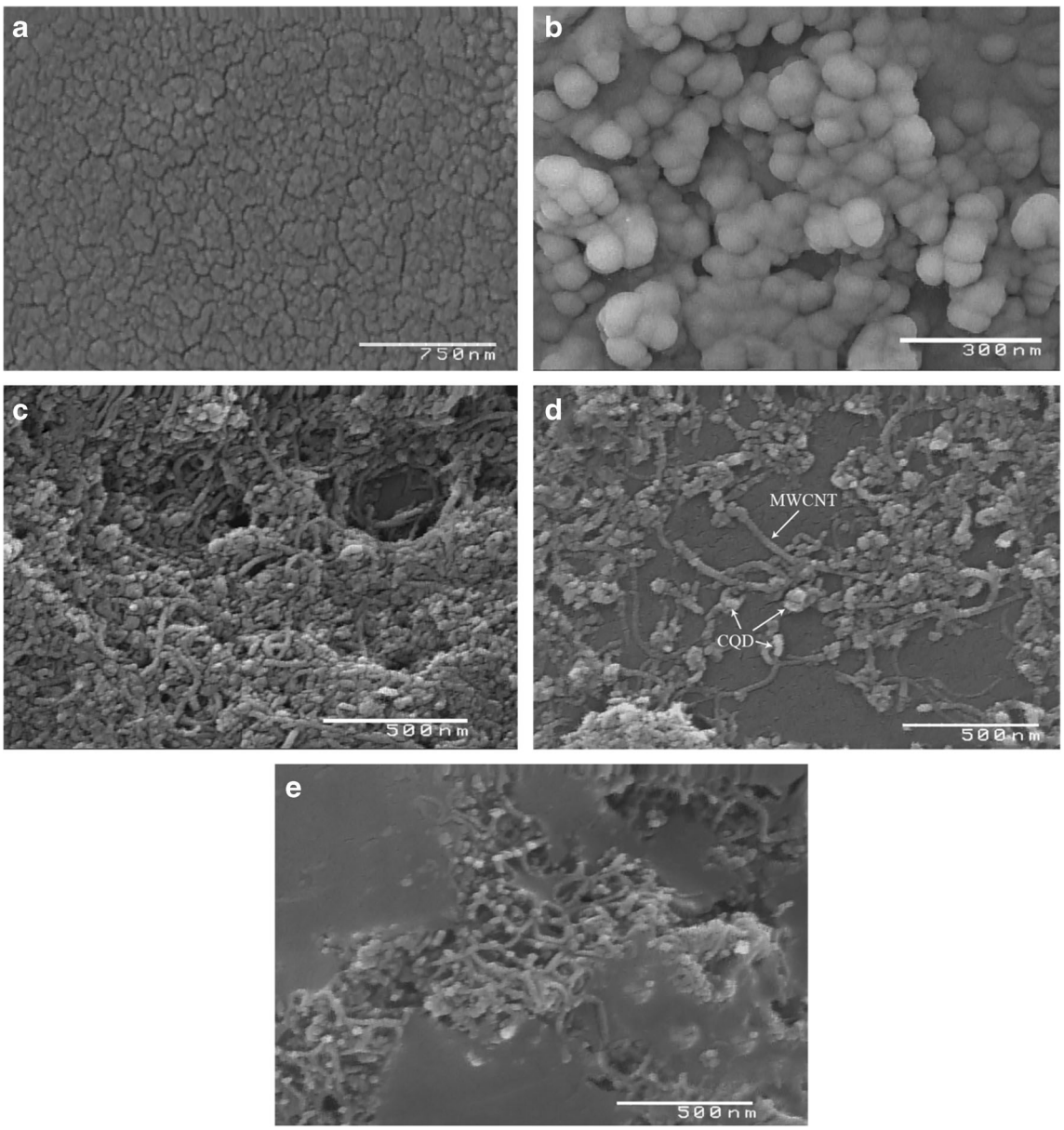

Fig. 1 FE-SEM images of **a** Unmodified GCE, **b** CQD/PDDA, **c** MWCNT/PDDA, **d** MWCNT/PDDA/CQD, and **e** MWCNT/PDDA/CQD/APT

Evaluation of the electrochemical properties of CQD/PDDA, MWCNT/PDDA, and MWCNT/PDDA/CQD nanocomposites

In this section, for each step, the CV, EIS, and DPV techniques are applied to investigate electrochemical properties of mentioned different nanocomposites. Figure 2a shows the DPVs of 2.5 mmol L^{-1} $[Fe(CN)_6]^{3-/4-}$ (1:1) and 0.1 mol L^{-1} KCl in 10 mM TE buffer on the different GCE covered with CQD/PDDA, MWCNT/PDDA, and MWCNT/PDDA/CQD nanocomposites. The unmodified GCE has a discrete peak (trace a). After covering the electrode surface with CQD/PDDA, the current response clearly increases (trace b). However, MWCNT/PDDA enhanced the electron transfer characteristics and increase the GCE surface (trace c). This led to an increase in the current response. By modifying the electrode with MWCNT/PDDA/CQD, current response increases even more (trace d) in than other previous statuses. This nanocomposite with high conductivity increases the electron-transfer ability and the GCE surface. The outcome of this section shows that the MWCNT/PDDA/CQD electrochemical properties are better than CQD/PDDA and MWCNT/PDDA nanocomposites. It should be noted that the results of electrochemical analysis relating to only PDDA were not discussed in this study because the results did not show a sensible change in electrochemical measurements in comparison with unmodified GCE. Additionally, CV outputs (Fig. 2b) confirm the differential pulse voltammetry outputs acquired under similar conditions. After that, EIS measurements are acquired for different nano-modified GCEs under similar conditions. This study showed that, after coating MWCNT/PDDA, the value of R_{ct} is sharply reduced, in comparison with bare and CQD/PDDA modified electrode, which can be attributed to the great conducting capability of MWCNTs. Moreover, as presented in the Fig. 2c, after coating the GCE with MWCNT/PDDA/CQDs, the R_{ct} decreases a little in comparison with MWCNT/PDDA modified electrode due to the presence of CQDs.

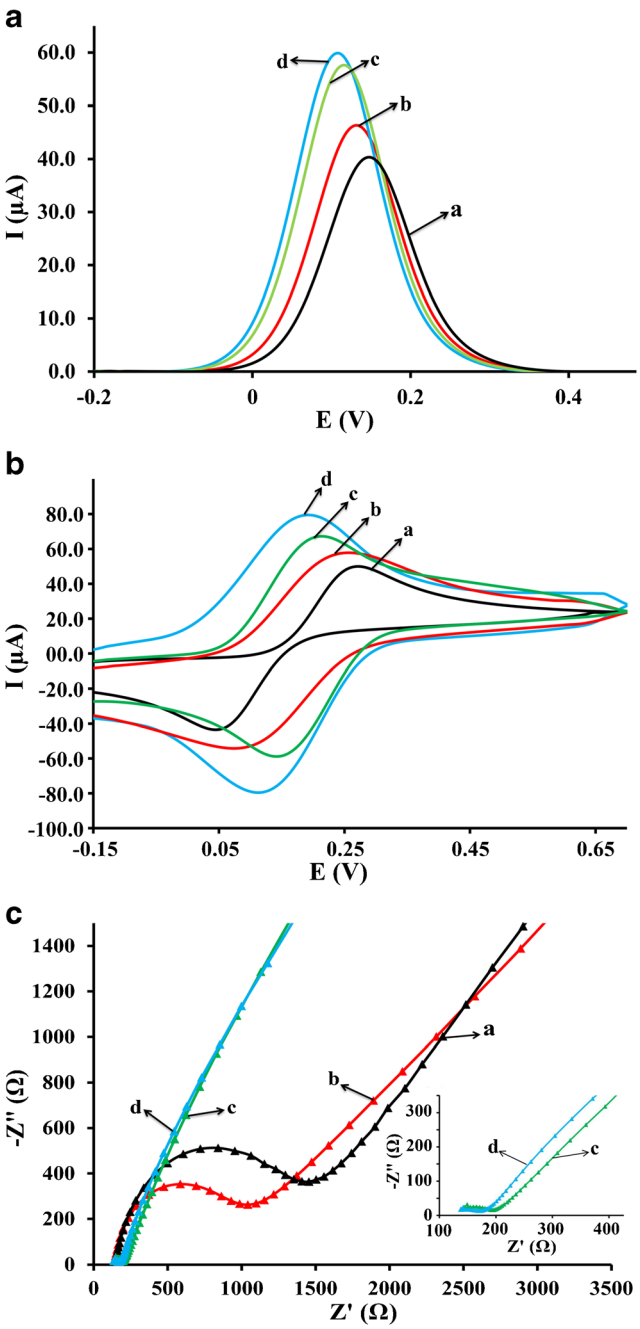

Fig. 2 **a** DPV, **b** CV, **c** EIS curves of (a) unmodified GCE, and modified GCE with (b) CQD/PDDA, (c) MWCNT/PDDA, (d) MWCNT/PDDA/CQD nanocomposites in a solution containing 2.5 mmol L^{-1} $[Fe(CN)_6]^{3-/4-}$ (1:1) mixture and 0.1 mol L^{-1} KCl in TE buffer (Inset in Fig. **c** is the zoom of trace c and d)

Lysozyme detection

EIS and DPV values of samples at different steps and lysozyme detection were obtained using 2.5 mmol L^{-1} $[Fe(CN)_6]^{3-/4-}$ (1:1) mixture as a redox probe and 0.1 mol L^{-1} KCl in TE buffer.

The aptamer immobilization process on the nanomaterials modified GCE surface restricts the access of electrons to the transducer surface, which leads to the low efficiency of electron transfer. Subsequently, this process leads to the increase of R_{ct} in the EIS and decrease of peak current (I_p) in the DPV measurements. Moreover, after lysozyme detection with GCE-MWCNT/PDDA/CQD/aptamer, I_p decreases continuously and R_{ct} increases because lysozyme additionally restricts the access of electrons to the surface of nano-modified GCE.

The MWCNT/PDDA, CQD/PDDA, and MWCNT/PDDA/CQD were used for the fabrication of the lysozyme aptasensor. The amount of immobilized aotamer (APT) and the performance of lysozyme detection on the modified GCE with these nanocomposites were also compared with

each other. Figure 3a and b shows variation of lysozyme detection performance on the different modified GCE surfaces by R_{ct} and I_p values. The differences between R_{ct} and I_p values (ΔR and ΔI) are considered as the main responses for after and before preparation of a new adhesive layer. As for lysozyme assay based on CQD/PDDA, MWCNT/PDDA and MWCNT/PDDA/CQD nanocomposites, the outcomes demonstrate that the ΔI values after lysozyme detection ($C_{lysozyme} = 0.05$ nmol L^{-1}) are 2.60, 3.71, and 10.31 μA, respectively. Besides, the values of the ΔR are 139.1, 177.9, and 724.6 Ω, respectively, for the three above-mentioned nanocomposites. The considerable increase in the values of ΔR and ΔI at MWCNT/PDDA/CQD, compared to other nano-modified GCE, is appropriate for the lysozyme identification. For more details about DPV and EIS behaviors of the three aforementioned nanocomposites, see Fig. 4a-f.

Figures 3 and 4 show that, after the immobilization of aptamer on the MWCNT/PDDA/CQD and catching the lysozyme, the biggest increase and decrease can be seen in R_{ct} and I_p, respectively. These results show the better immobilization of aptamer due to the existence of synthesized CQDs with carboxyl functional group on MWCNTs. This result suggests a novel prospect for applying such films in the detection of protein.

Figure 5a shows the DPV voltammograms for different lysozyme concentrations. As shown in this figure, the peak currents decrease as the analyte concentration increases. Fig. 5b presents the calibration plot.

The peak current is inversely proportional to the lysozyme concentrations in the wide range of 50 fmol L^{-1} to 10 nmol L^{-1}. The detection limit for lysozyme concentration is 12.9 fmol L^{-1} at a signal-to-noise ratio of 3. The regression equation is $\Delta I = 2.8156 \lg c + 14.371$ with the estimated detection limit of 12.9 fmol L^{-1} at 3 S_b/m (where m is the slope of the corresponding calibration curve and S_b is the standard deviation of the blank). In addition, sensitivity, which is equal to m, is 2.8156 μA/nM. The peak currents are equivalent to the logarithm of lysozyme concentration in the wide range of measurement from 50 fmol L^{-1} to 10 nmol L^{-1}, as shown in Fig. 5b (Inset). The lysozyme assay developed in this study is compared with previous electrochemical aptasensors for lysozyme detection in terms of aptamer construction and detection techniques (Table 1). According to Table 1, the LOD and linear range of lysozyme detection can be better than that of other electrochemical aptasensors, which have been presented up to now.

Storage stability and repeatability

In the practical application of the detection of the lysozyme protein, the storage stability of the modified GCE is an important issue. To assess the stability of the GCE-MWCNT/PDDA/CQD/aptamer, Fig. 5c is provided to present the time-dependency of the relative current response change, related to the original signal of 0.05 nmol L^{-1} lysozyme on the first day of measurement. The GCEswere kept in dry conditions at temperature of 4 °C between each measurement on different days. The results show that, in lysozyme presence, after one month, the signal for 0.05 nmol L^{-1} lysozyme is 89% of the original signal (Fig. 5c). This outcome reveals that the GCE has good stability.

The repeatability of the applied aptasensor is also important in the assay of protein. Ten parallel-prepared GCE-MWCNT/PDDA/CQD/aptamers were applied for identifying 0.003 nmol L^{-1} lysozyme (See Table S1, Section S2.2). The signals of ten modified GCEs for detection of 0.003 nmol L^{-1} lysozyme are shown in Table S1. A Relative Standard Deviation (RSD) of 4.9% is also evaluated for the value of ΔI.

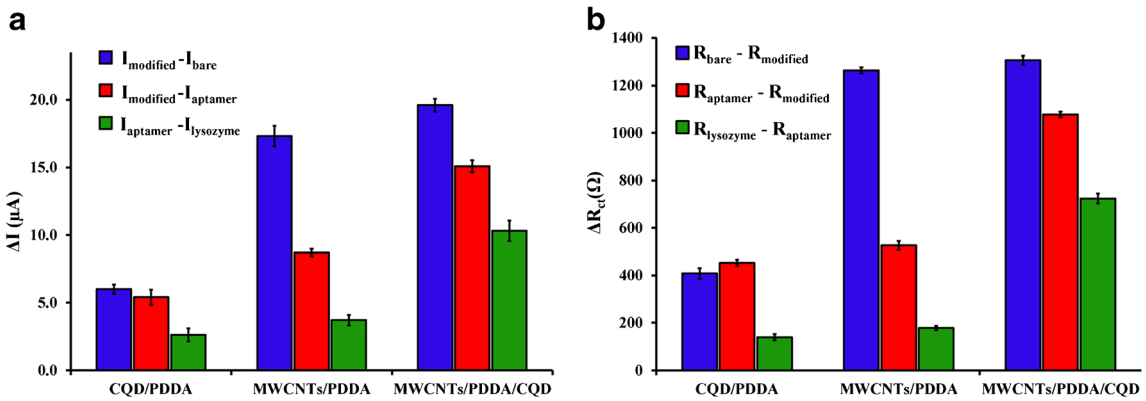

Fig. 3 **a** Ip and **b** R_{ct} variation for each step in detection of lysozyme was measured via prepared aptasensor, in which CQD/PDDA, MWCNT/PDDA, and MWCNT/PDDA/CQD were applied as sensitive layers

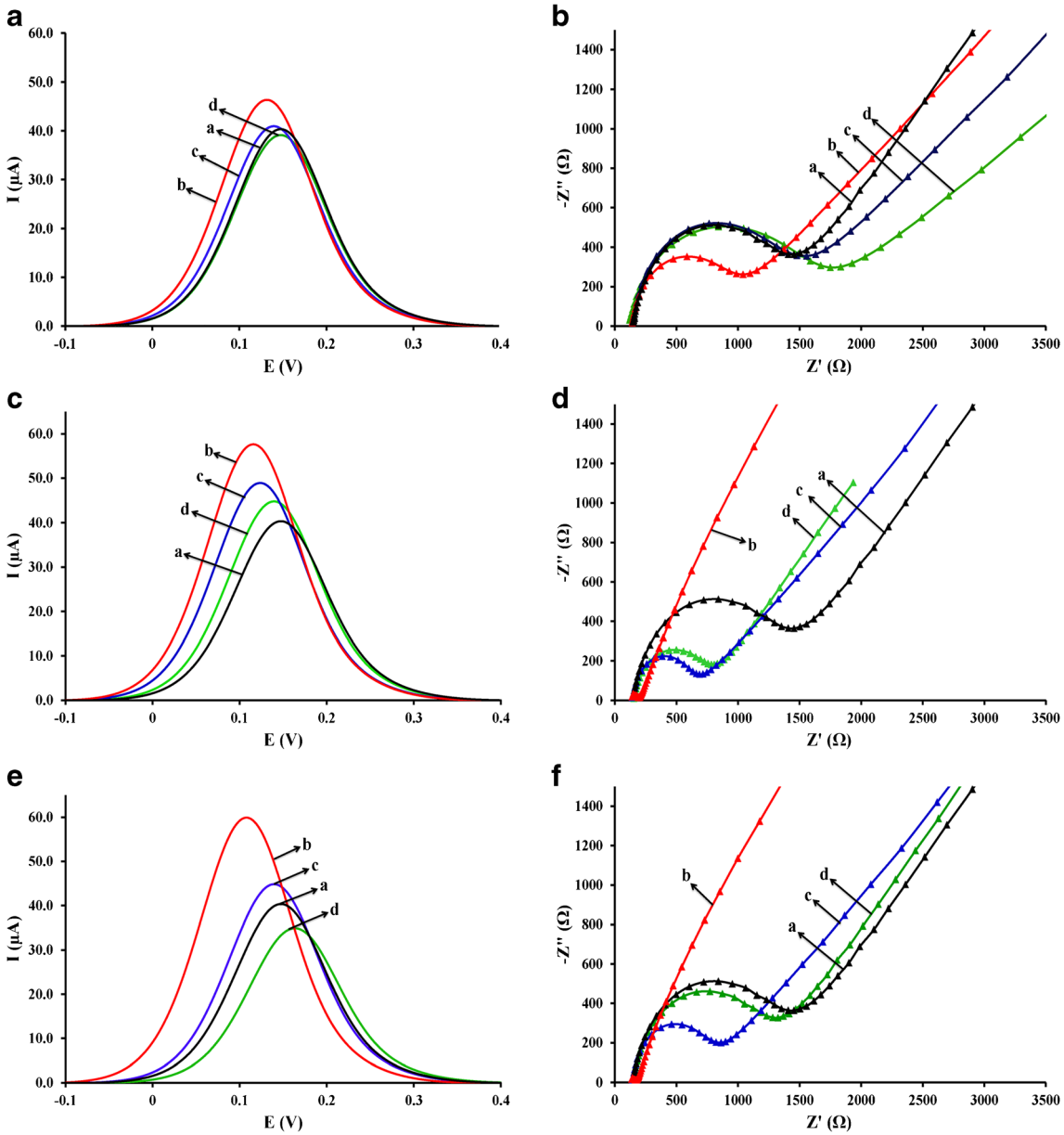

Fig. 4 **a** DPV and **b** EIS curves of (a) unmodified GCE, (b) nano-modified GCE of CQD/PDDA, (c) immobilized aptamer on the nano-modified GCE of CQD/PDDA, and (d) aptamer fitted to lysozyme (0.05 nmol L^{-1}). **c** DPV and **d** EIS curves of (a) unmodified GCE, (b) GCE modified with MWCNT/PDDA, (c) immobilized aptamer on the GCE modified with MWCNT/PDDA, and (d) aptamer fitted to lysozyme (0.05 nmol L^{-1}). **e** DPV and **f** EIS curves of (a) unmodified GCE, (b) GCE modified with MWCNT/PDDA/CQD, (c) immobilized aptamer on the GCE modified with MWCNT/PDDA/CQD, and (d) aptamer fitted to lysozyme (0.05 nmol L^{-1}) .DPV and EIS curves acquired in a solution containing 2.5 mmol L^{-1} $[Fe(CN)_6]^{3-/4-}$ (1:1) mixture and 0.1 mol L^{-1} KCl in TE buffer (pH 7.4)

Specificity of the assay

In this section, some proteins being in the same family as lysozyme, like thrombin, BHb, human IgG, and BSA were used to evaluate selectivity. In addition, they were applied to determine any probable non-specific adsorption of other proteins onto the nano-modified GCE. The mixture of these proteins with lysozyme has been tested under the same experimental conditions. As observed in Fig. 5d, the peak current of the anti-lysozyme GCE-MWCNT/PDDA/CQD/aptamer related to the addition of human IgG (0.1 nmol L^{-1}), BSA (0.3 nmol L^{-1}), BHb (0.3 nmol L^{-1}), and thrombin (0.03 nmol L^{-1}) does not show considerable changes in the current,

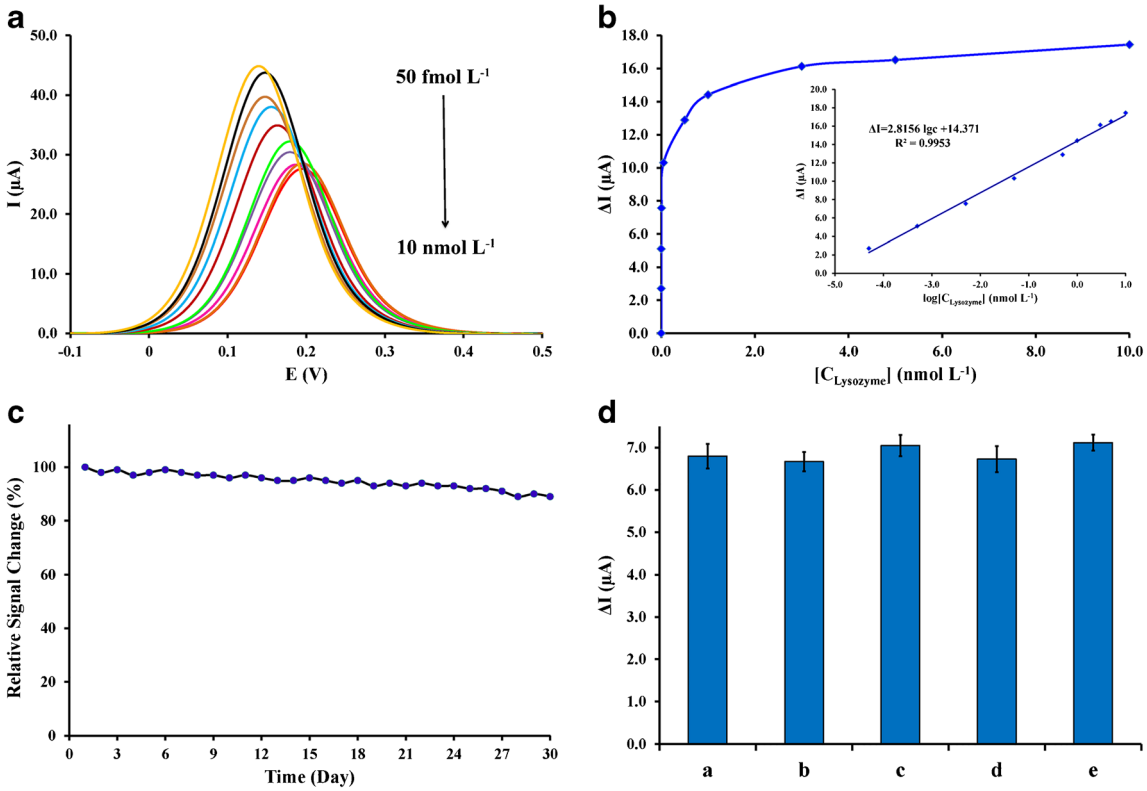

Fig. 5 **a** DPV voltammograms of the GCE modified with MWCNT/PDDA/CQD/aptamer for different concentrations of lysozyme within 50 fmol L^{-1} – 10 nmol L^{-1} with scan rate 100 mVs^{-1}, **b** calibration curve for ΔI and (Inset) ΔI vs. log($C_{lysozyme}$, nmol L^{-1}), **c** Time dependency of relative current response change connecting to the original signal at 5.0 nmol L^{-1} lysozyme on the first day of measurement, **d** Peak current response to (a) 0.003 nmol L^{-1} lysozyme, mixtures of 0.003 nmol L^{-1} lysozyme with (b) 0.3 nmol L^{-1} BSA, (c) 0.1 nmol L^{-1} human IgG, (d) 0.3 nmol L^{-1} BHb, (e) 0.03 nmol L^{-1} thrombin, respectively, ($n = 3$)

Table 1 Comparison of developed electrochemical aptasensors for detection of lysozyme

Method	Electrode & material	LOD	Linear range	Sample	RSD%	References
SWV	GCE/Au/(Fc-cDNA/LBA TWJ)	0.2 nM	0.2–100 nM	–	7.90	[8]
SWV	SPCE/AuNPs/LBA	21 fM	0.07–3.4 pM	Egg white	4.20	[26]
SWV	GCE/THH Au NCs/APT	0.1 pM	0.1 pM–10 nM	Egg white, serum	7.70	[8]
LSW	Au/cDNA/LBA	1 pM	1.0 pM–1.1 nM	Egg white	4.20	[8]
EIS	rGO-AuNP/chit-AuNP/MWCNT-AuNP	9 fM	0.02 to 250 pM	Saliva, urine	3.9	[22]
EIS	Au/cDNA/LBA	70 pM	0.2–4.0 nM	–	3.70	[8]
EIS	LBA–GR–GCE	6 fM	0.01–0.5 pM	Saliva, Egg white	–	[29]
EIS	SPCE/LBA1 and LBA2	25 nM	0.025–0.8 μM	Wine	3.80	[8]
EIS	GCE/ AuNPs/erGO	0.06 pM	1.0 to 104.3 pM	Serum	–	[27]
EIS	Fe2O3-GR-GCE/LBA	11.1 pM	35 pM–350 nM	–	4.48	[8]
CV	Au/LBA/TCA/AuNPs/cDNA	0.1 pM	5 pM–1 nM	Egg white	4.30	[8]
DPV	Au/CD/DLAP1 + DLAP2	64 pM	100–1000 pM	Serum	–	[8]
DPV	GR-GCE/LBA	0.08 nM	0.2 nM–1040 nM	–	4.23	[8]
DPV	GCE/O-GNs/LBA	1 pM	5.0 pM–0.7 nM	–	–	[8]
DPV	SPCE/LBA/Lysozyme/B-AB/SA-ALP	4.3 fM	5 f. to 5 nM	wine	5.5	[14]
DPV	Au-Cu2O/rGO/PpPG	0.06 nM	0.1 nM −200 nM	saliva, plasma, urine	4.8	[24]
DPV	GCE/ AuNPs/erGO	0.24 pM	9.6–205.5 pM	Serum	5.8	[27]
DPV	GCE-MWCNT/PDDA/CQD	12.9 fM	50 f. −10 nM	Egg white, Serum, urine	4.9	This work

Table 2 Recovery measurements of lysozyme for real sample analysis in the presence of applied GCE-MWCNT/PDDA/CQD/aptamer

Samples	Detected (nM)	Spiked lysozyme (nM)	Found (nM)	Recovery (%)	RSD(%)
Egg white	2.23 ± 0.07	1.00	3.26 ± 0.34	102.03	5.01
		3.00	5.16 ± 0.31	97.67	3.56
		5.00	7.29 ± 0.39	101.20	4.61
Serum	4.61 ± 0.09	1.00	5.59 ± 0.21	98.04	4.86
		3.00	7.69 ± 0.38	102.67	4.73
		5.00	9.44 ± 0.34	96.60	5.09
Urine	0.52 ± 0.05	1.00	1.49 ± 0.26	97.01	4.11
		3.00	3.56 ± 0.33	101.30	3.72
		5.00	5.45 ± 0.28	98.60	4.54

compared to the response to lysozyme (0.003 nmol L^{-1}). This suggests that the electrode has excellent selectivity in detecting between lysozyme and other different proteins.

Application to lysozyme detection in real samples

In this section, the lysozyme content in egg white, serum, and urine of healthy people was tested to examine the feasibility of applying the sensor in the real sample analysis by DPV after preparation (Table 2). For this purpose, 1.0 g of egg white was diluted 1000 times in TE buffer; serum and urine were provided from healthy persons and diluted 15 and 5 times in TE buffer, respectively. Then, the modified GCE was immersed into the each of the real samples for 1.5 h. The lysozyme concentrations are 2.23 ± 0.07 nM, 4.61 ± 0.09 nM, and 0.52 ± 0.05 nM ($n = 4$) for egg white, serum, and urine, respectively. These measurements are located into normal range of the reported values [8]. By applying analytical recovery experiments, the accuracy of the assay was tested, as shown in Table 2. According to the standard addition method, the percentage of spiked recoveries changes from 96.60 to 102.67. The results confirm the efficiency of this technique for lysozyme analysis in real and biological samples.

Conclusions

This study has developed a novel electrochemical lysozyme assay based on the use of a MWCNT/PDDA/CQD nanocomposite. In this scheme, the aptamer on adsorbent layer catches the target lysozyme on the electrode interface. This process makes a barrier for electrons and restricts electron transfer; therefore, resulting in a decrease in DPV peak current. The results demonstrate that the immobilized amount of aptamer on the modified GCE has increased. This method has several advantages in comparison with other electrochemical aptasensors for biomolecule (aptamer) immobilization, including (i) the existence of large amounts of hydroxy, carboxy, and amino functional groups in synthetic CQD and functionalized MWCNTs, and positively charged PDDA; (ii) fast electron-transfer kinetics which is due to the presence of MWCNTs; (iii) high surface-to-volume ratio in the presence of CQDs and MWCNTs. Although the fabrication of nanoparticles and CQDs is not straightforward and fabrication has complex stages, they have a lot of advantages compared to other electrochemical aptasensors, like great stability, selectivity, and sensitivity. In our perception, this approach is a powerful and selective tool for improving and developing novel electrochemical aptasensors.

Acknowledgements The authors wish to thank the Center of Excellence in Sensor and Green Chemistry and Research Council of Isfahan University of Technology (IUT), and the Iranian Nanotechnology Initiative Council for their support.

Compliance with ethical standards The author(s) declare that they have no competing interests.

References

1. Setford SJ, White SF, Bolbot JA (2002) Measurement of protein using an electrochemical bi-enzyme sensor. Biosens Bioelectron 17:79–86. https://doi.org/10.1016/S0956-5663(01)00264-0
2. Gianazza E, Tremoli E, Banfi C (2014) The selected reaction monitoring/multiple reaction monitoring-based mass spectrometry approach for the accurate quantitation of proteins: clinical applications in the cardiovascular diseases. Expert Rev Proteom 11:771–788. https://doi.org/10.1586/14789450.2014.947966
3. Zhang LX, Cao YR, Xiao H, Liu XP, Liu SR, Meng QH, Fan L, Cao C (2016) Leverage principle of retardation signal in titration of double protein via chip moving reaction boundary electrophoresis.

Biosens Bioelectron 77:284–291. https://doi.org/10.1016/j.bios.2015.09.001
4. Yoo G, Bong JH, Kim S, Jose J, Pyun JC (2014) Microarray based on autodisplayed Ro proteins for medical diagnosis of systemic lupus erythematosus (SLE). Biosens Bioelectron 57:213–218. https://doi.org/10.1016/j.bios.2014.02.018
5. Goda T, Higashi D, Matsumoto A, Hoshi T, Sawaguchi T, Miyahara Y (2015) Dual aptamer-immobilized surfaces for improved affinity through multiple target binding in potentiometric thrombin biosensing. Biosens Bioelectron 73:174–180. https://doi.org/10.1016/j.bios.2015.05.067
6. Liu DY, Zhao Y, He XW, Yin XB (2011) Electrochemical aptasensor using the tripropylamine oxidation to probe intramolecular displacement between target and complementary nucleotide for protein array. Biosens Bioelectron 26:2905–2910. https://doi.org/10.1016/j.bios.2010.11.035
7. Cheng AKH, Ge BX, HZ Y (2007) Aptamer-based biosensors for label-free voltammetric detection of lysozyme. Anal Chem 79:5158–5164. https://doi.org/10.1021/ac062214q
8. Vasilescu A, Wang Q, Li M, Boukherroub R, Szunerits S (2016) Aptamer-based electrochemical sensing of lysozyme. Chem Aust 4:10–30. https://doi.org/10.3390/chemosensors4020010
9. Weth F, Schroeder T, Buxtorf UP, Lebensm Z (1988) Determination of lysozyme content in eggs and egg products using SDS-gel electrophoresis. Eur Food Res Technol 187:541–545. https://doi.org/10.1007/BF01042386
10. Daeschel MA, Musafija-Jeknic T, Wu Y, Bizzarri D, Villa A (2002) High-performance liquid chromatography analysis of lysozyme in wine. Am J Enol Vitic 53:154–157
11. Lacorn MGC, Haas-Lauterbach S, Immer U (2010) Sensitive lysozyme testing in red and white wine using the ridascreen fast lysozyme ELISA. Bulletin de l'OIV 83:507–511
12. Zhao Y, Chen H, Chen Q, Qi Y, Yang F, Tang J, He P, Zhang F (2014) Ultrasensitive and signal-on electrochemiluminescence aptasensor using the multi-tris(bipyridine) ruthenium(II)-β-cyclodextrin complexes. Chin J Chem 32(11):1161–1168. https://doi.org/10.1002/cjoc.201400511
13. Vasilescu A, Gaspar S, Mihai I, Tache A, Litescu SC (2013) Development of a label-free aptasensor for monitoring the self-association of lysozyme. Analyst 138:3530–3537. https://doi.org/10.1039/C3AN00229B
14. Ocana C, Hayat A, Mishra R, Vasilescu A, del Valle M, Marty J-L (2015) A novel electrochemical aptamer-antibody sandwich assay for lysozyme detection. Analyst (Cambridge, UK) 140(12):4148–4153. https://doi.org/10.1039/C5AN00243E
15. Mir M, Vreeke M, Katakis I (2006) Different strategies to develop an electrochemical thrombin aptasensor. Electrochem Commun 8:505–511. https://doi.org/10.1016/j.elecom.2005.12.022
16. Wang S, Hu X, Tan L, Liao Q, Chen Z (2016) Colorimetric detection of lysozyme based on its effect on the growth of gold nanoparticles induced by the reaction of chloroauric acid and hydroxylamine. Microchim Acta 183:3135–3141. https://doi.org/10.1007/s00604-016-1969-2
17. Yang L, Fung C, Cho EJ, Ellington AD (2007) Real-time rolling circle amplification for protein detection. Anal Chem 79:3320–3329. https://doi.org/10.1021/ac062186b
18. Zheng B, Cheng S, Liu W, Lam MHW, Liang H (2013) Small organic molecules detection based on aptamer-modified gold nanoparticles-enhanced quartz crystal microbalance with dissipation biosensor. Anal Biochem 438:144–149. https://doi.org/10.1016/j.ab.2013.03.030
19. Villamizar RA, Maroto A, Rius FX, Inza I, Figueras MJ (2008) Fast detection of salmonella Infantis with carbon nanotube field effect transistors. Biosens Bioelectron 24:279–283. https://doi.org/10.1016/j.bios.2008.03.046
20. Bahsi ZB, Buyukaksoy A, Olmezcan SM, Simsek F, Aslan MH, Oral AY (2009) A novel label-free optical biosensor using synthetic oligonucleotides from E. coli O157: H7: elementary sensitivity tests. Sensors 9:4890–4900. https://doi.org/10.3390/s90604890
21. Gehring AG, SI T (2005) Enzyme-linked immunomagnetic electrochemical detection of live Escherichia coli O157: H7 in apple juice. Food Prot 68:146–149. https://doi.org/10.4315/0362-028X-68.1.146
22. Heydari-Bafrooei E, Askari S (2017) Ultrasensitive aptasensing of lysozyme by exploiting the synergistic effect of gold nanoparticle-modified reduced graphene oxide and MWCNTs in a chitosan matrix. Microchim Acta 184:3405–3413. https://doi.org/10.1007/s00604-017-2356-3
23. Iliuk AB, Hu L, Tao W (2011) Aptamer in bioanalytical applications. Anal Chem 83:4440–4452. https://doi.org/10.1021/ac201057w
24. Fang S, Dong X, Ji H, Liu S, Yan F, Peng D, Zhang Z (2016) Electrochemical aptasensor for lysozyme based on a gold electrode modified with a nanocomposite consisting of reduced graphene oxide, cuprous oxide, and plasma-polymerized propargylamine. Microchim Acta 183:633–642. https://doi.org/10.1007/s00604-015-1675-5
25. Ensafi AA, Jamei HR, Heydari-Bafrooei E, Rezaei B (2014) Development of a voltammetric procedure based on DNA interaction for sensitive monitoring of chrysoidine, a banned dye, in foods and textile effluents. Sensors Actuators B 202:224–231. https://doi.org/10.1016/j.snb.2014.05.001
26. Xie D, Li C, Shangguan L, Qi H, Xue D, Gao Q, Zhang C (2014) Click chemistry-assisted self-assembly of DNA aptamer on gold nanoparticles-modified screen-printed carbon electrodes for label-free electrochemical aptasensor. Sensors Actuators B 192:558–564. https://doi.org/10.1016/j.snb.2013.11.038
27. Shamsipur M, Farzin L, Tabrizi MA (2016) Ultrasensitive aptamer-based on-off assay for lysozyme using a glassy carbon electrode modified with gold nanoparticles and electrochemically reduced graphene oxide. Microchim Acta 183:2733–2743. https://doi.org/10.1007/s00604-016-1920-6
28. Ensafi AA, Jamei HR, Heydari-Bafrooei E, Rezaei B (2016) Electrochemical study of quinone redox cycling: a novel application of DNA-based biosensors for monitoring biochemical reactions. Bioelectrochemistry 111:15–22. https://doi.org/10.1016/j.bioelechem.2016.04.008
29. Xiao Y, Wang Y, Wu M, Ma X, Yang X (2013) Graphene-based lysozyme binding aptamer nanocomposite for label-free and sensitive lysozyme sensing. J Electroanal Chem 702:49–55. https://doi.org/10.1016/j.jelechem.2013.05.010
30. Xu J, Wang Y, Hu S (2017) Nanocomposites of graphene and graphene oxides: synthesis, molecular functionalization and application in electrochemical sensors and biosensors. A review. Microchim Acta 184(1):1–44
31. Gao X, Cui Y, Levenson M, Chung LW, Nie S (2004) In vivo cancer targeting and imaging with semiconductor quantum dots. Nat Biotechnol 22:969–976
32. Lim SY, Shen W, Gao Z (2015) Carbon quantum dots and their applications. Chem Soc Rev 44:362–381. https://doi.org/10.1039/C4CS00269E
33. Qu D, Zheng M, Du P, Zhou Y, Zhang L, Li D, Tan H, Zhao Z, Xie Z, Sun Z (2013) Highly luminescent S, N co-doped graphene quantum dots with broad visible absorption bands for visible light photocatalysts. Nano 5:12272–12277. https://doi.org/10.1039/C3NR04402E
34. Yang X, Yang X, Li Z, Li S, Han Y, Chen Y, Bu X, Su C, Xu H, Jiang Y, Lin Q (2015) Photoluminescent carbon dots synthesized by microwave treatment for selective image of cancer cells. J Colloid Interface Sci 456:1–6. https://doi.org/10.1016/j.jcis.2015.06.002